Consistency of the recent ATLAS $Z + E_T^{\rm miss}$ excess in a simplified GGM model

Ben Allanach,[1] Are Raklev,[2] and Anders Kvellestad[2]

[1] *DAMTP, CMS, Wilberforce Road, University of Cambridge, Cambridge, CB3 0WA, United Kingdom*
[2] *Department of Physics, University of Oslo, N-0316 Oslo, Norway*

ATLAS recently reported a 3σ excess in a leptonic-$Z + E_T^{\rm miss}$ channel. This was interpreted in the literature in a simplified General Gauge Mediation model containing a gluino, a higgsino next-to-lightest supersymmetric particle (NLSP) and a gravitino lightest supersymmetric particle (LSP). We test the consistency of this explanation in lieu of the results of the corresponding search in CMS, and other LHC searches for New Physics. Due to non-decoupling effects from squarks the parameter space of these models is split into two regions; in one region additional leptons via top quark production is expected, while the other region sees a large probability for zero-lepton events. After combining the relevant constraints we find that these models cannot explain the ATLAS excess.

PACS numbers: 12.60.Jy, 13.15.tg, 14.80.Ly

arXiv:1504.02752v2 [hep-ph] 20 Apr 2015

I. INTRODUCTION

A recent ATLAS search for beyond the standard model physics in a channel with two leptons, consistent with the production of a Z-boson, large missing transverse momentum ($E_T^{\rm miss}$), and at least two jets, reports a 3σ excess [1] for 20.3 fb^{-1} of integrated luminosity at a center of mass energy of 8 TeV. The other general purpose LHC experiment, CMS, has reported on a similar search, also with the full Run-I data set [2], seeing no excess. However, the cuts used in the two searches are different, and the observed ATLAS excess may *a priori* be consistent with the CMS results. Also, because the cuts are different, for some particular interpretation in terms of a new physics model one expects the predicted signal rates in each analysis to depend upon the signal kinematics. Hence, the relative number of predicted signal events in ATLAS as compared to CMS will depend in general upon the assumed interpretation, as well as on its parameters.

In this article we investigate the consistency of the ATLAS excess with the CMS analysis, and with other searches at the LHC, for a General Gauge Mediation (GGM) model with a gravitino LSP [3]. The simplified model used here is inspired by [4], and contains only three free parameters: the gaugino mass M_3, fixing the gluino mass, $\tan\beta$, the ratio of the two higgs field vacuum expectation values, and μ, the superpotential parameter, giving the mass of the higgsino NLSP, as well as one additional neutralino and one chargino, both dominantly higgsino. The excess can then be interpreted as stemming from gluino pair production and the decay chain $\tilde{g} \to qq\tilde{\chi}_1^0 \to qqZ\tilde{G}$, depicted in Fig. 1, with a leptonic Z-decay. In doing so we follow the model chosen by ATLAS to interpret the results of their analysis.

As the leptonic branching ratio of the Z is small, this model may also come in to conflict with recent searches for supersymmetry (SUSY) via jets and missing energy channels. This was briefly commented on in [5], but no detailed analysis of the parameter space was performed, and the article goes on to interpret the ATLAS results in an alternative model with Zs coming from the decay $\tilde{\chi}_2^0 \to Z\tilde{\chi}_1^0$. The ATLAS excess was also interpreted in [6], using two benchmark points in a GGM model with properties very similar to the model used by ATLAS, and in [7], in the context of a composite Higgs/Randall Sundrum model, with heavy Kaluza-Klein gluon resonances decaying to vector-like quarks.

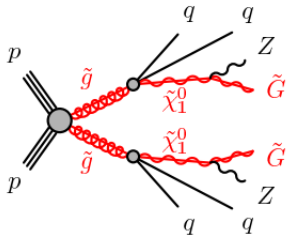


FIG. 1. Hypothesized GGM decay mode contributing to the ATLAS excess.

II. MODEL

For the model used in the ATLAS interpretation the remaining minimal supersymmetric standard model (MSSM) parameters were set as follows: the gaugino soft masses $M_1 = M_2 = 1$ TeV, the sfermion soft masses $m_{\tilde{f}} = 1.5$ TeV, and a gravitino mass light enough for the NLSP decays to be prompt. With $m_{\tilde{q}} = 1.5$ TeV, squark–gluino production dominates over gluino pair production for gluino masses above ~ 1 TeV. Squark–squark production would dominate sparticle production for high enough gluino masses. Also, with $M_1 = M_2 = 1$ TeV more complicated decay chains open up for gluinos in this mass range, and the NLSP will no longer be dominantly higgsino for values of μ close to 1 TeV.[1]

[1] Alternatively, MSSM scenarios with a wino (or bino) NLSP could be considered, however, they have $BR(\tilde{\chi}_1^0 \to \gamma\tilde{G}) > 0.23\,(0.77)$ [8], which should be easy to exclude from $\gamma + E_T^{\rm miss}$ searches.

In order to explore a wider range of μ and M_3 values without introducing such complications in the phenomenology we adopt a simpler model with $M_1 = M_2 = 1.5$ TeV and sfermions completely decoupled at $m_{\tilde{f}} = 4.5$ TeV, keeping in mind that lowering the squark mass scale generally will lead to stronger bounds on the model. The mass parameters are defined at a scale of $\sqrt{m_{\tilde{t}_1} m_{\tilde{t}_2}} \sim 4.5$ TeV.

The gravitino mass is given by the scale of SUSY breaking, but must be very light for the NLSP to decay promptly; we set it to be effectively zero for the collider simulation. All results are presented for $\tan\beta = 1.5$ and $\tan\beta = 30$. The choice of low $\tan\beta$ is made in order to maximize the branching ratio $\tilde{\chi}_1^0 \to Z\tilde{G}$, which is in competition with $\tilde{\chi}_1^0 \to h\tilde{G}$, and to a smaller extent $\tilde{\chi}_1^0 \to \gamma\tilde{G}$. For low values of $\tan\beta$, $\mu > 0$ and a higgsino NLSP, this is approximately 100% [8–10]. Increasing $\tan\beta$ will decrease the signal. The two values used thus explore different parts of the parameter space.

The lightest higgs mass is simply set to the experimentally measured value of $m_h = 125.09 \pm 0.24$ GeV [11] by assuming extra operators in the higgs sector, *e.g.* by using dimension-5 operators as proposed in [12].

The relative squark masses (and to a smaller extent the value of M_1 and M_2) determine the branching ratio of the gluino decay into the various quark flavours. Since the NLSP is dominantly higgsino there will necessarily be large branching ratios into third generation quarks. When these are kinematically forbidden, the loop induced decays $\tilde{g} \to g\tilde{\chi}_{1,2}^0$ become important. Due to the importance of decays involving third generation quarks, $\tan\beta$ also affects the gluino branching ratios. Further complicating matters is the existence of multiple higgsinos at roughly the same mass ($\tilde{\chi}_1^0$, $\tilde{\chi}_2^0$ and $\tilde{\chi}_1^\pm$)[2]. In Fig. 2 we show the branching ratios of the gluino calculated using `SUSYHIT 1.4` [15], as a function of $\Delta m = m_{\tilde{g}} - m_{\tilde{\chi}_1^0}$ for $\tan\beta = 1.5$ (solid lines) and $\tan\beta = 30$ (dashed lines). The gluino mass is fixed at $m_{\tilde{g}} = 900$ GeV and the other parameters are as given above.

We see that at least one top quark will be produced per event on average even down to $\Delta m \sim 350$ GeV, where the proximity of the $\tilde{g} \to tb\chi_1^\pm$ threshold becomes important. For $\tan\beta = 30$ we get a sizeable contribution from the decays $\tilde{g} \to b\bar{b}\tilde{\chi}_{1,2}^0$, reducing somewhat the production of top quarks at high Δm. We find that lowering M_1 and/or M_2 down to the gluino mass changes little: there is a slight increase in the first and second generation quark decays versus the gluino loop decay below the $tb\chi_1^\pm$ threshold, but no significant impact above $\Delta m \sim 350$ GeV. This ensures the presence of a significant number of events with additional leptons from leptonic top decays, which we will see have an impact on the allowed

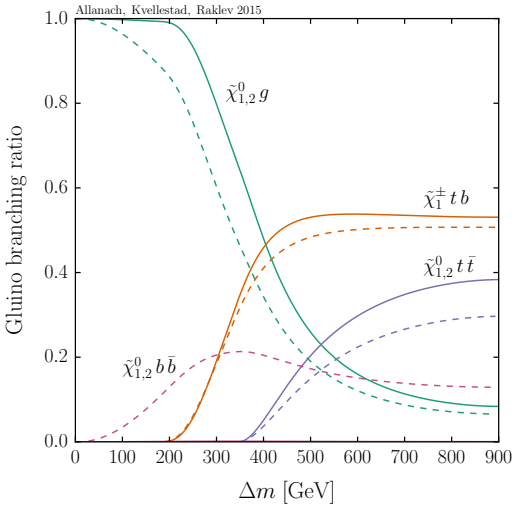


FIG. 2. Branching ratios for the gluino as a function of the gluino–neutralino mass difference with $\tan\beta = 1.5$ (solid lines) $\tan\beta = 30$ (dashed lines). The gluino mass is fixed at $m_{\tilde{g}} = 900$ GeV. Some lines are not visible because they are at very low values of the gluino branching ratio.

parameter space of the model. The decays to first and second generation quarks are heavily suppressed.

The ATLAS analysis assumed equal branching fractions of $\tilde{g} \to qq\tilde{\chi}_1^0$ for $q = u, d, c, s$, ignoring the heavy quark decays. This simplifying assumption has relatively little impact on their analysis and the bounds set because of the focus on leptons from the Z boson. However, the structure of GGM predicts generic sum rules on the sfermion soft masses [3],

$$m_Q^2 - 2m_U^2 + m_D^2 - m_L^2 + m_E^2 = 0 \quad (1)$$

$$2m_Q^2 - m_U^2 - m_D^2 - 2m_L^2 + m_E^2 = 0, \quad (2)$$

which makes decoupling only the third generation squarks challenging.[3] One is faced with the choice of either making the phenomenological assumption that the sum rules are broken somehow, increasing the number of free soft sfermion mass parameters in the model, and requiring an explanation of why the third generation masses are significantly heavier, *e.g.* one could speculate that something along the lines of higgsed gauge mediation [16] could work.[4] Or, to reduce the number of top quarks produced, one can at best decouple all squarks except the lightest bottom squarks by an appropriate choice

[2] We note that a co-NLSP scenario is unlikely for higgsinos. This would require relatively small but negative M_1 values and large M_2, see [13, 14].

[3] Technically the ATLAS model does not fulfil these sum rules, however, a slight modification of the soft mass parameters would.

[4] With first and second generation sfermions at 1.5 TeV, the third generation sfermions must be raised to ~ 5 TeV for the gluino branching ratios to light quarks to equal those to third generation quarks.

observed	29
background	10.6±3.2
number of sigma	3.0
s (95% CL)	7.1-31.8

TABLE I. Summary of `ATLAS_onZ` constraints, showing the observed number of events, the number of expected Standard Model events inferred from data, the number of sigma the excess corresponds to and the 95% CL constraint upon a putative number of signal events s. The first three data are taken from Ref. [1], whereas we infer the bound on s ourselves (see text).

of the soft masses, however, the decay $\tilde{g} \to tb\chi_1^\pm$ remains. Neither seems very consistent with the simple model of ATLAS. As a result we will here include gluino decays to top and bottom quarks in the model.

III. SCAN AND SIMULATIONS

We perform a grid scan over the range 0–1500 GeV in μ and M_3, using a step size of 15 GeV in both directions. At each step we calculate the resulting sparticle spectrum using `SOFTSUSY 3.5.1` [17] and the sparticle branching ratios with `SUSYHIT 1.4` [15]. Spectrum and decay information is communicated via the SUSY Les Houches Accord [18], using `PySLHA` [19]. For all parameter points we check that $m_{\tilde{g}} > m_{\tilde{\chi}_1^0}$, and that the NLSP is mostly higgsino (more than 0.90). At each point we generate 100 000 SUSY Monte Carlo events with gluino pair production using `Pythia 8.186` [20, 21]. The cross sections used are based on `Prospino` [22], using the `NLLfast` software including also NLL re-summation of soft gluon emission [23–26]. These events are then propagated through our implementations of several collider analyses, detailed below.

The ATLAS analysis with the excess requires two leading opposite sign same flavor (OSSF) leptons with $p_T > 25, 10$ GeV and invariant mass $81 < m_{ll} < 101$ GeV, a minimum missing transverse energy of $E_T^{\rm miss} > 225$ GeV, at least two jets, and total transverse energy $H_T > 600$ GeV, where H_T is given as the scalar sum of the transverse momenta of the two leading leptons and all accepted jets. Jets are reconstructed with the anti-k_T algorithm [27] using `FastJet` [28], with a jet radius parameter of $R = 0.4$, and are required to have $p_T > 35$ GeV and lie within $|\eta| < 2.5$. In the following we will denote the signal region with the sum of ee and $\mu\mu$ events as `ATLAS_onZ`. We summarize the ATLAS measurements in Table I. In order to calculate a constraint upon the number of non-Standard Model signal events s, we profile over a Gaussian background rate, see Section IV, but otherwise use Poisson statistics. If other combined constraints predict an `ATLAS_onZ` signal rate outside of this range, we shall conclude that they are incompatible with the signal at the 95% CL.

The on-Z CMS analysis [2], here called `CMS_onZ`, requires a leading pair of opposite sign same flavor leptons satisfying $p_T > 20$ GeV and $81 < m_{ll} < 101$ GeV. Three signal regions are constructed, covering the ranges 100–200 GeV, 200–300 GeV and > 300 GeV in $E_T^{\rm miss}$, all requiring at least three jets with $p_T > 40$ GeV and $|\eta| < 3.0$. For jet reconstruction the anti-k_T algorithm with $R = 0.5$ is used. A notable difference with respect to the event selection in `ATLAS_onZ` is that no cut on H_T is applied. While there are some details of the original analysis which are difficult to reproduce outside of the experimental collaborations, *e.g.* trigger efficiencies, by simulating models similar to those used for interpretation in `ATLAS_onZ` and `CMS_onZ` we have checked that our implementations reproduce the observed limits to within theoretical uncertainties, under the assumptions made.

In addition to the leptonic-Z + $E_T^{\rm miss}$ analyses from CMS and ATLAS, the scenario used here could be constrained by other searches involving leptons. This includes three and four lepton final states where extra leptons are produced in leptonic top decays, or from two chains with Zs. The latter is heavily suppressed by the leptonic branching ratio of the Z, down to $\sim 7\%$ of the number of events with a single leptonically decaying Z, thus of the order of two events could be expected for the given luminosity, depending on the exact cuts of such an analysis.

We check the most relevant searches which are the ATLAS stop search with leptons `ATLAS_stop_L100` [29], and the CMS multi-lepton search with three or four leptons, `CMS_multilepton` [30]. From the analysis in `ATLAS_stop_L100` we include the signal region `L100` requiring exactly two opposite-sign leptons with $p_T > 25, 10$ GeV, at least two jets with $p_T > 100, 50$ GeV, a 'stransverse mass' $m_{T2} > 100$ GeV and an invariant mass m_{ll} for the two leptons outside the range 71–111 GeV. For the GGM model studied here, the cut on m_{ll} means that `ATLAS_stop_L100` is mainly sensitive to events where neither of the two Zs decay leptonically.

The CMS multi-lepton search requires at least three isolated leptons with $p_T > 20, 10, 10$ GeV within $|\eta| < 2.4$. Jets are subject to the requirements $p_T > 30$ GeV and $|\eta| < 2.5$. Accepted events are divided into a large number of signal regions based on the number of opposite-sign same-flavour lepton pairs, $E_T^{\rm miss}$, the presence of a OSSF lepton pair with an invariant mass in the 75–105 GeV range, the scalar sum of jet p_Ts and the number of tagged b-jets. Due to an overlap between `CMS_onZ` and the most relevant signal regions in `CMS_multilepton`, in the combination we use `CMS_multilepton` for parameter regions where the gluino–neutralino mass difference Δm is larger than 500 GeV and `CMS_onZ` for mass differences smaller than this. A choice like this is necessary in order to have statistically independent signal regions when we do not have the information to take into account the correlations. As can be seen from Fig. 2, the choice ensures that `CMS_multilepton` is only applied in the region of parameter space where additional leptons can be

expected due to a sizeable production of top quarks.

Given the small leptonic branching ratios of W and Z, the GGM scenario studied can also be constrained from searches for zero-lepton final states. We include the signal region `3j` from the ATLAS search for final states with jets and missing energy [31], here called `ATLAS_jMET_3j`. Besides a lepton veto, this signal region requires at least three jets with $p_T > 130, 60, 60$ GeV and $|\eta| < 2.8$, missing energy $E_T^{\rm miss} > 160$ GeV and an 'effective mass' $m_{\rm eff} > 2200$ GeV. Also, the missing energy is required to account for at least 30% of the effective mass combination of $E_T^{\rm miss}$ and the three leading jet p_Ts.

No significant excesses are seen in either of these searches. For all three searches we have checked, as above, that we can reproduce the relevant limits on SUSY interpretations presented by the experiments.

IV. STATISTICS

In order to combine the results from all the analyses, each independent signal region i is assigned a likelihood $\mathcal{L}_i$ consisting of a Poisson factor for the total event count and a Gaussian for modelling the background uncertainty:

$$\mathcal{L}_i(s_i, b_i) = \text{Pois}(n_i|s_i + b_i) \times \text{Gauss}(b_{m_i}|b_i, \sigma_{b_i}). \quad (3)$$

Here n_i is the observed number of events, s_i and b_i are the expected number of signal and background events, and b_{m_i} is the observed background measurement with an expected standard deviation σ_{b_i}. Inserting the observed values for n_i, b_{m_i} and σ_{b_i} we are left with a likelihood function for the two parameters s_i and b_i. While s_i will be a function of the SUSY parameters μ and M_3, b_i is an unknown nuisance parameter which we eliminate by profiling $\mathcal{L}_i$ over b_i. With all the $\mathcal{L}_i$ coming from independent signal regions, the combined likelihood is then simply given by

$$\mathcal{L}(\mathbf{s}) = \prod_i \mathcal{L}_i(s_i, \hat{\hat{b}}_i), \quad (4)$$

where the double hat indicates that we have maximized $\mathcal{L}_i(s_i, b_i)$ over b_i subject to a fixed value of s_i.

For any given parameter point in μ and M_3, the signal expectation values $\mathbf{s}$ are in principle fully determined. In order to set limits in the model parameter space we introduce a common signal strength parameter μ_s such that the expected signal yield in signal region i is $\mu_s s_i$. Points in the SUSY parameter space for which the upper limit on μ_s is found to be less than 1 will be excluded at the confidence level chosen for the test.

For every choice of the SUSY parameters we now have a single-parameter likelihood function $\mathcal{L}(\mu_s) \equiv \mathcal{L}(\mu_s \mathbf{s})$. From the likelihood ratio

$$\lambda(\mu_s) = \frac{\mathcal{L}(\mu_s)}{\mathcal{L}(\hat{\mu}_s)}, \quad (5)$$

we construct a test statistic q given by

$$q = \begin{cases} -2\ln\lambda(\mu_s) & \hat{\mu}_s \le \mu_s \\ 0 & \hat{\mu}_s > \mu_s, \end{cases} \quad (6)$$

where $\hat{\mu}_s$ is the value of μ_s that maximizes $\mathcal{L}(\mu_s)$, *i.e.* the signal strength value preferred by the observed data. Higher values of q correspond to increasing disagreement between data and the hypothesized value of μ_s, but only in the direction of $\mu_s > \hat{\mu}_s$. For a given μ_s the observed value $q_{\rm obs}$ of q is calculated from the data. The p-value for this observation is then found from

$$p_{\mu_s} = \int_{q_{\rm obs}}^{\infty} f(q|\mu_s)\, dq, \quad (7)$$

where $f(q|\mu_s)$ is the pdf of q. To determine p_{μ_s} we make use of the asymptotic limit in which $f(q|\mu_s)$ is given by a 'half chi-square' distribution, *i.e.* an equally-weighted sum of a delta function at zero and a chi-square distribution for one degree of freedom [32]. The 95% CL$_s$ [33] upper limit on μ_s is the highest value of μ_s satisfying

$$\frac{p_{\mu_s}}{1 - p_0} \ge 0.05, \quad (8)$$

where p_0 is the p-value for the test statistic

$$q_0 = \begin{cases} -2\ln\lambda(0) & \hat{\mu}_s \ge 0 \\ 0 & \hat{\mu}_s < 0, \end{cases} \quad (9)$$

used to test the level of disagreement between data and the background-only hypothesis.

V. RESULTS

We show the 95% CL allowed region for the 3σ `ATLAS_onZ` excess in Fig. 3 for $\tan\beta = 1.5, 30$ as the lighter band. The 95% CL$_s$ excluded regions from the other searches are overlaid, and for reference the two ATLAS benchmark points at $(m_{\tilde{g}}, m_{\tilde{\chi}_1^0}) = (700, 200)$ GeV and $(900, 600)$ GeV, $\tan\beta = 1.5$, are indicated with white diamond markers. It is clear from the figure that all points explaining the `ATLAS_onZ` excess for either value of $\tan\beta$ fall afoul of at least one of the other searches. Indeed, `CMS_onZ` alone is already incompatible with the excess at the 95% CL$_s$ level except for two small regions. One region, around $m_{\tilde{\chi}_1^0} \approx 950$ GeV, $m_{\tilde{g}} \approx 980$ GeV which is anyway well excluded by the `ATLAS_jMET` searches. The other region, including the point $m_{\tilde{\chi}_1^0} = 190$ GeV, $m_{\tilde{g}} = 930$ GeV is excluded by `CMS_multilepton`. When $\tan\beta$ is changed, the exclusion contours move somewhat in gluino and lightest neutralino mass, but the qualitative conclusions remain unchanged.

Given the tension between the other searches and the `ATLAS_onZ` excess, we now combine the `CMS_onZ` exclusion with various other searches to see what the combined

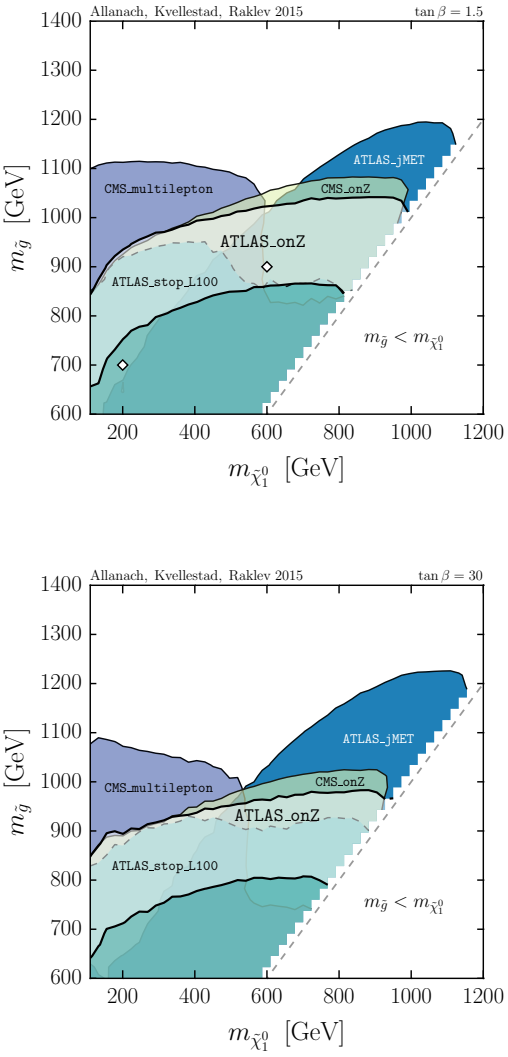


FIG. 3. The band in the $(m_{\tilde{\chi}_1^0}, m_{\tilde{g}})$–plane preferred by ATLAS_onZ at 95% CL (lighter region), compared to the coloured 95% CL_s exclusion contours from CMS_onZ, ATLAS_stop_L100, CMS_multilepton and ATLAS_jMET for $\tan\beta = 1.5$ (top), $\tan\beta = 30$ (bottom). The ATLAS_stop_L100 exclusion region boundary is shown as a dashed line. Two ATLAS benchmark points are indicated with white diamond markers.

data set predicts for the number of signal events in the excess. The 95% CL_s bound in the $(m_{\tilde{\chi}_1^0}, m_{\tilde{g}})$–plane resulting from combining ATLAS_onZ and CMS_onZ is shown in Fig. 4. Here the white contour depicts the limit obtained for $\tan\beta = 1.5$, while the black contour is for $\tan\beta = 30$. Also shown are the bounds given a 20% systematic uncertainty on the cross section. The color map shows the predicted number of signal events for the ATLAS_onZ analysis in the scenario with $\tan\beta = 1.5$. Since the squarks are decoupled from gluino production here, the production cross section for the model is lower than the original ATLAS scenario. Still, both ATLAS benchmark points are excluded at the 95% confidence level from the combination of ATLAS_onZ and CMS_onZ alone. On the other hand, there are still some points left allowed at the 95% CL that predict an ATLAS_onZ signal rate of up to 13(12) for $\tan\beta = 1.5(30)$. These are *within* the 95% CL signal rate region of $7.1 - 31.8$ and so are still compatible with the ATLAS_onZ signal at the 95% CL.

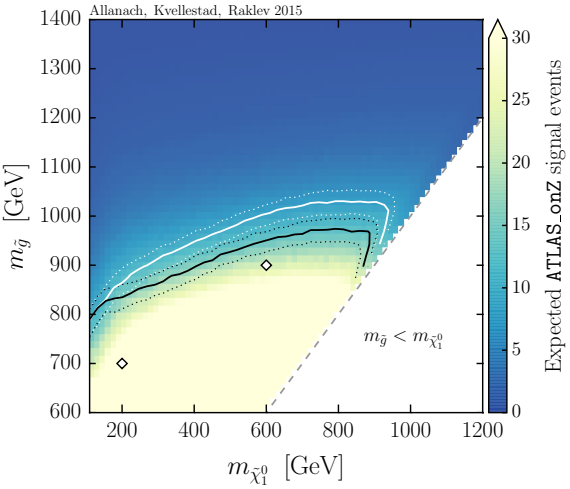


FIG. 4. The 95% CL_s exclusion curves in the $(m_{\tilde{\chi}_1^0}, m_{\tilde{g}})$–plane for $\tan\beta = 1.5$ (white) and $\tan\beta = 30$ (black), using both the ATLAS_onZ and CMS_onZ signal regions. The color map shows the expected number of ATLAS_onZ signal events for the $\tan\beta = 1.5$ scenario. The two ATLAS benchmark points are indicated with white diamond markers. The region below each curve is excluded by the combination. ATLAS_onZ signal events are constrained to be below 13(12) at the 95% CL for $\tan\beta = 1.5(30)$.

If we add on the contributions from ATLAS_stop_L100 and CMS_multilepton the resulting 95% CL_s bound is shown in Fig. 5. As expected, the exclusion limits are improved in the regions of large gluino–neutralino mass difference, where the production of additional leptons through top quarks is significant. The slight dip in the contour at $(m_{\tilde{g}}, m_{\tilde{\chi}_1^0}) \sim (1000, 500)$ GeV is where the domains of the CMS_multilepton and CMS_onZ analyses meet. In the region of small gluino–neutralino mass difference the limit remains approximately unchanged, and the combined allowed region predicts up to 13(11) ATLAS_onZ signal events for $\tan\beta = 1.5(30)$, still consistent with the $7.1 - 31.8$ 95% CL constraint.

The final exclusion limit, obtained after including also ATLAS_jMET_3j, is shown in Fig. 6. Due to the lepton veto in this analysis, the exclusion limit is mainly strengthened in the region with gluino–neutralino mass differences less than 400 GeV, where the main source of leptons is through the small leptonic branching ratio of the Zs. With $\tan\beta = 30$ this effect is further enhanced by

the reduced branching ratio into Zs. We note that gluino masses below 1 TeV are fully excluded for both values of $\tan\beta$, and the remaining allowed parameter space has a maximum of 6 expected signal events for ATLAS_onZ, which is far from explaining the observed excess.

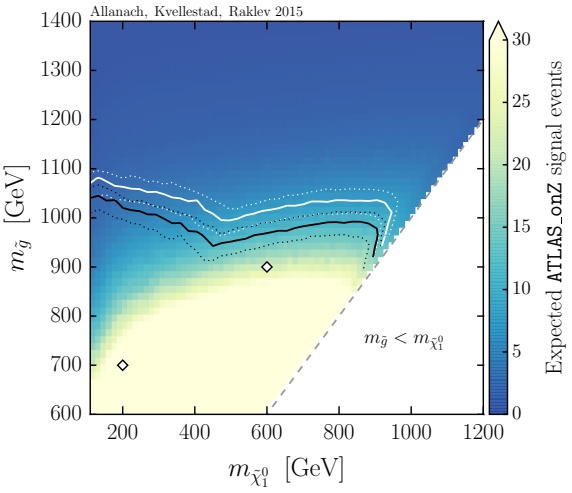


FIG. 5. The 95% CL_s exclusion curves in the $(m_{\tilde{\chi}_1^0}, m_{\tilde{g}})$–plane from combining ATLAS_onZ, CMS_onZ, ATLAS_stop_L100 and CMS_multilepton. The color map shows the expected number of ATLAS_onZ signal events for the $\tan\beta = 1.5$ scenario. The two ATLAS benchmark points are indicated with white diamond markers. The region below each curve is excluded by the combination. ATLAS_onZ signal events are constrained to be below 13(11) at the 95% CL for $\tan\beta = 1.5(30)$.

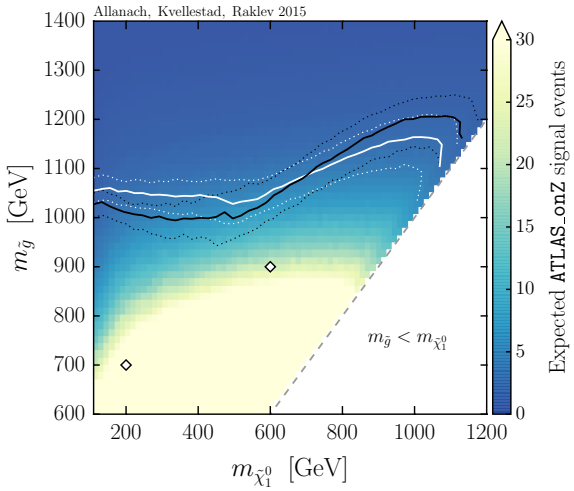


FIG. 6. The 95% CL_s exclusion curves in the $(m_{\tilde{\chi}_1^0}, m_{\tilde{g}})$–plane from combining all collider searches detailed in the text. The color map shows the expected number of ATLAS_onZ signal events for the $\tan\beta = 1.5$ scenario. The two ATLAS benchmark points are indicated with white diamond markers. The region below each curve is excluded by the combination. ATLAS_onZ signal events are constrained to be below 6(5) at the 95% CL for $\tan\beta = 1.5(30)$.

The observed excess in ATLAS_onZ was also recently interpreted within a GGM framework in [6], where two new benchmark points are presented. The main difference with respect to the ATLAS scenario is heavier squarks, and that the lightest neutralino is a wino–bino mixture. The first point, referred to as GGM1, has $m_{\tilde{g}} = 1088$ GeV, $m_{\tilde{\chi}_1^0} = 428$ GeV and squark masses around 2800 GeV. The second point, GGM2, has a higher production cross section due to lighter gluinos and squarks, at 911 GeV and ~ 2400 GeV, respectively. Combining the collider constraints considered here we find that GGM2 is excluded at the 95% confidence level, while GGM1 escapes exclusion. However, it should be noted that GGM1 predicts only ~ 3 signal events for ATLAS_onZ[5].

One may ask: can one tweak the simplified model in order to squeeze around the constraints? In our analysis, we have set the simplified model up in order to *maximize* the ATLAS_onZ region compared to the other constraining searches. If $\tan\beta$ is increased further, the ATLAS_onZ signal decreases for the same gluino/lightest neutralino masses. Thus, these would have to be lowered in order to get a signal to fit, and such lighter sparticles would suffer more from the other searches. If we were to make squarks lighter, although the ATLAS_onZ signal would increase for the same gluino/lightest neutralino masses, the ATLAS_jMET constraints would become *much* stronger. In any case, CMS_onZ is in tension with nearly all of the ATLAS_onZ parameter space, and this is unlikely to change. The CMS_multilepton constraint is mainly due to events with one leptonically decaying Z-boson plus additional leptons from decaying top quarks, predicted by the signal model due to the higgsino nature of the neutralino. If the model is manipulated to reduce the production of such additional leptons, the weakening of the CMS_multilepton constraint will be compensated by a corresponding strengthening of ATLAS_jMET as more events will pass the lepton veto. Thus, although we have not exhaustively covered the full multi-dimensional MSSM plus light gravitino space, there are good grounds for expecting that our conclusions — that the ATLAS_onZ excess is incompatible with other searches at the 95% CL for GGM-type models — also apply to the full MSSM space.

[5] We note that this is in slight disagreement with the simulation in [6], which finds 6 ± 1 predicted signal events for GGM1. However, this discrepancy does not change the conclusion.

VI. CONCLUSIONS

In conclusion, we have seen that a simplified GGM model with only M_3 and μ as free parameters, and with $\tilde{g}$, higgsino $\tilde{\chi}_1^0$, $\tilde{\chi}_2^0$ and $\tilde{\chi}_1^\pm$, and a gravitino LSP as the only sparticles produced at the LHC, cannot explain the ATLAS excess reported in [1] when faced with results from other current new physics searches. Strong bounds on the model that can be set from other leptonic searches are due to the higgsino nature of the NLSP, leading to the production of top quarks with leptonic decays. Zero-lepton searches also provide strong constraints in the parameter regions where leptons are mainly produced through the small leptonic branching ratio of the Z. Tension between `ATLAS_onZ` and the other relevant searches is evident in Fig. 3. A combined fit to all constraints, *including the excess*, at the 95% CL predicts less than 6 signal events in the `ATLAS_onZ` search region, compared to 7.1-31.8 being inferred from the `ATLAS_onZ` search region alone.

ACKNOWLEDGMENTS

This work has been partially supported by STFC grant ST/L000385/1. We thank the Cambridge SUSY Working Group for stimulating discussions. The CPU intensive parts of this work was performed on the Abel Cluster, owned by the University of Oslo and the Norwegian metacenter for High Performance Computing (NOTUR), and operated by the Research Computing Services group at USIT, the University of Oslo IT-department. The computing time was given by NOTUR allocation NN9284K, financed through the Research Council of Norway.

[1] G. Aad *et al.* (ATLAS), (2015), arXiv:1503.03290 [hep-ex].
[2] V. Khachatryan *et al.* (CMS), (2015), arXiv:1502.06031 [hep-ex].
[3] P. Meade, N. Seiberg, and D. Shih, Prog.Theor.Phys.Suppl. **177**, 143 (2009), arXiv:0801.3278 [hep-ph].
[4] J. T. Ruderman and D. Shih, JHEP **1208**, 159 (2012), arXiv:1103.6083 [hep-ph].
[5] U. Ellwanger, (2015), arXiv:1504.02244 [hep-ph].
[6] G. Barenboim, J. Bernabeu, V. Mitsou, E. Romero, E. Torro, *et al.*, (2015), arXiv:1503.04184 [hep-ph].
[7] N. Vignaroli, (2015), arXiv:1504.01768 [hep-ph].
[8] P. Meade, M. Reece, and D. Shih, JHEP **1005**, 105 (2010), arXiv:0911.4130 [hep-ph].
[9] S. Ambrosanio, G. L. Kane, G. D. Kribs, S. P. Martin, and S. Mrenna, Phys.Rev. **D54**, 5395 (1996), arXiv:hep-ph/9605398 [hep-ph].
[10] S. Dimopoulos, S. D. Thomas, and J. D. Wells, Nucl.Phys. **B488**, 39 (1997), arXiv:hep-ph/9609434 [hep-ph].
[11] G. Aad *et al.* (CMS s), (2015), arXiv:1503.07589 [hep-ex].
[12] M. Dine, N. Seiberg, and S. Thomas, Phys.Rev. **D76**, 095004 (2007), arXiv:0707.0005 [hep-ph].
[13] G. F. Giudice and A. Pomarol, Phys.Lett. **B372**, 253 (1996), arXiv:hep-ph/9512337 [hep-ph].
[14] N.-E. Bomark, A. Kvellestad, S. Lola, P. Osland, and A. Raklev, JHEP **1405**, 007 (2014), arXiv:1310.2788 [hep-ph].
[15] A. Djouadi, M. Muhlleitner, and M. Spira, Acta Phys.Polon. **B38**, 635 (2007), arXiv:hep-ph/0609292 [hep-ph].
[16] N. Craig, M. McCullough, and J. Thaler, JHEP **1203**, 049 (2012), arXiv:1201.2179 [hep-ph].
[17] B. Allanach, Comput.Phys.Commun. **143**, 305 (2002), arXiv:hep-ph/0104145 [hep-ph].
[18] P. Z. Skands, B. Allanach, H. Baer, C. Balazs, G. Belanger, *et al.*, JHEP **0407**, 036 (2004), arXiv:hep-ph/0311123 [hep-ph].
[19] A. Buckley, (2013), arXiv:1305.4194 [hep-ph].
[20] T. Sjostrand, S. Mrenna, and P. Z. Skands, JHEP **0605**, 026 (2006), arXiv:hep-ph/0603175 [hep-ph].
[21] T. Sjostrand, S. Mrenna, and P. Z. Skands, Comput.Phys.Commun. **178**, 852 (2008), arXiv:0710.3820 [hep-ph].
[22] W. Beenakker, R. Hopker, M. Spira, and P. Zerwas, Nucl.Phys. **B492**, 51 (1997), arXiv:hep-ph/9610490 [hep-ph].
[23] A. Kulesza and L. Motyka, Phys.Rev.Lett. **102**, 111802 (2009), arXiv:0807.2405 [hep-ph].
[24] A. Kulesza and L. Motyka, Phys.Rev. **D80**, 095004 (2009), arXiv:0905.4749 [hep-ph].
[25] W. Beenakker, S. Brensing, M. Kramer, A. Kulesza, E. Laenen, *et al.*, JHEP **0912**, 041 (2009), arXiv:0909.4418 [hep-ph].
[26] W. Beenakker, S. Brensing, M. Kramer, A. Kulesza, E. Laenen, *et al.*, Int.J.Mod.Phys. **A26**, 2637 (2011), arXiv:1105.1110 [hep-ph].
[27] M. Cacciari, G. P. Salam, and G. Soyez, JHEP **0804**, 063 (2008), arXiv:0802.1189 [hep-ph].
[28] M. Cacciari, G. P. Salam, and G. Soyez, Eur.Phys.J. **C72**, 1896 (2012), arXiv:1111.6097 [hep-ph].
[29] G. Aad *et al.* (ATLAS), JHEP **1406**, 124 (2014), arXiv:1403.4853 [hep-ex].
[30] S. Chatrchyan *et al.* (CMS), Phys.Rev. **D90**, 032006 (2014), arXiv:1404.5801 [hep-ex].
[31] G. Aad *et al.* (ATLAS Collaboration), (2014), arXiv:1405.7875 [hep-ex].
[32] G. Cowan, K. Cranmer, E. Gross, and O. Vitells, Eur.Phys.J. **C71**, 1554 (2011), arXiv:1007.1727 [physics.data-an].
[33] A. L. Read, J.Phys. **G28**, 2693 (2002).